Multiscale Green's-function method for modeling point defects and extended defects in anisotropic solids: Application to a vacancy and free surface in copper

V. K. Tewary*

Materials Reliability Division, National Institute of Standards and Technology, Boulder, Colorado 80305, USA

The elastic response of a vacancy in a semi-infinite fcc copper lattice containing a free surface is calculated by using a new multiscale Green's function method. The method treats the lattice distortion near the vacancy at the atomistic level and the free surface at the macroscopic continuum level in the same formalism. The lattice is modeled using the lattice statics Green's function that fully accounts for the discrete atomistic structure of the lattice and can model a large crystallite containing a million atoms without excessive CPU effort. The method is especially useful for modeling the elastic response of nanocrystals containing point defects in which surfaces and interfaces play important roles. The method bridges the length scales seamlessly by relating the microscopic lattice distortion near a point defect to measurable macroscopic parameters of the solid such as the strain and the displacement field at a free surface. Using the interatomic potential derived by Cleri and Rosato, the lattice distortion, relaxation energy, and relaxation volume due to a vacancy are calculated in an otherwise perfect copper lattice for a million-atom model containing a free (100) surface. The calculated value of the relaxation volume is in excellent agreement with the observed value. Numerical results are also presented for the strain and the displacement fields at the free surface due to a vacancy and the interaction energy between a vacancy and the free surface in anisotropic semi-infinite copper.

I. INTRODUCTION

We describe a multiscale Green's function (MSGF) method to model a vacancy in a semi-infinite fcc copper lattice containing a free surface at two length scales: Atomistic and continuum. At the continuum scale, we calculate the strain and the displacement fields at the free surface due to a vacancy in the bulk and the elastic interaction energy between the vacancy and the free surface. At the atomistic scale, we calculate the lattice distortion, the relaxation energy and the relaxation volume due to the vacancy. These length scales are linked seamlessly in the MSGF method. The method fully accounts for the discrete structure of the lattice at the atomistic scale and the elastic anisotropy of the solid at the continuum scale.

A vacancy is an important point defect in a solid since it affects the mechanical as well as electrical properties of the solid. Since the strain and the displacement fields at the surface can be measured, these quantities can be useful for characterizing a vacancy and observing its physical effects on a solid. The elastic interaction energy gives the concentration of vacancies near the free surface, which is important for modeling diffusion and other related processes that are important for technological applications such as the stability and reliability of copper interconnects in devices.

The strain or the displacement fields are usually measured at or near a free surface. It is, therefore, important to model a vacancy and at least one free surface in the same formalism. The effect of other surfaces in the solid can be neglected if the vacancy is close to the surface where the measurements are made and other surfaces are far enough. The free surface also affects the displacement field due to the vacancy, which is responsible for the elastic interaction between the surface and the vacancy. Strain field due to a vacancy or any other

point defect in a semi-infinite solid containing a free surface can be calculated by using the continuum model Green's function[1,2] for a half-space solid. The continuum model has been quite successful in modeling extended defects such as free surfaces and interfaces.[3] However, it is well known that the continuum model is not a suitable representation[4-6] of the response of a solid near a point defect. It is necessary to account for the discrete structure of the lattice at least near the point defect and also include the effect of the free surface.

There are two techniques available in the literature for pure atomistic calculations of the properties of a vacancy or any point defect in an infinite lattice: One using the lattice statics Green's functions (LSGF)[6,7] and the other using molecular dynamics (MD)[8-13] (for review and other references, see Refs. 8 and 13). In both the techniques an infinite solid is represented by a finite crystallite with periodic boundary conditions. So far there have been no LSGF or MD calculations on a point defect in a semi-infinite solid, which account for a free surface in the solid as well as the discrete atomistic structure of the lattice near the point defect. These techniques have to be extended to multiscale systems that include extended defects such as free surfaces along with point defects.

The LSGF method has the advantage that it can model a large crystallite without excessive CPU requirements. For example, even a million-atom model requires only a few seconds of CPU time to calculate the LSGF on a standard 3 GHz desktop. A disadvantage of the LSGF method is that it does not account for nonlinear effects. In case of a single vacancy, the harmonic approximation is valid[4-6] and hence the LSGF method is applicable. On the other hand, the MD accounts for nonlinear response but is usually limited to small crystallites containing a few hundred atoms. Large crystallites can be modeled using MD only by using special techniques and massive CPU effort.[9]

In the MD model, the calculation of the energy of a vacancy converges within a few hundred atoms beyond which the energy is not sensitive to the size of the crystallite. So the MD model of a small crystallite containing a few hundred atoms is adequate for calculation of the formation energy of a vacancy. However, a small crystallite can not be used for calculations of strains which are defined by long range displacement fields. Atomic displacements beyond the range of the direct interaction from the vacancy contribute little to the formation energy of the vacancy[6] but are important for calculations of strain and surface effects. For calculation of the strain, therefore, it is necessary to use a very large crystallite which makes the MD model computationally inefficient. In contrast, the LSGF method is computationally very efficient for modeling large crystallites. We, therefore, adopt the LSGF method for multiscale modeling.

In this paper we describe a new multiscale Green's function (MSGF) method for modeling a point defect and a free surface in a semi-infinite solid. The MSGF method is an extension of the LSGF method. It fully accounts for the discrete atomistic structure of the solid near the point defect and uses the continuum model to include the effect of the free surface. The model is truly multiscale because it seamlessly links the response of the solid at the atomistic level to its response at the macro level. The method can be applied to any point defect and any extended defect in a general anisotropic solid.

The MSGF method bridges the length scales from the atomistic (subnano) to the continuum (macro) and thus directly relates the physical processes at the atomistic level to measurable macroscopic parameters. In order to see the importance of a multiscale formulation, consider, for example, the lattice distortion caused by a point defect in a solid. The lattice distortion is defined as the atomic displacements at discrete lattice sites. Experimentally one measures the strain near a free surface. Strain is a macroscopic quantity. It is a parameter of the continuum model defined in terms of derivatives of the continuous displacement field. It is, therefore, not strictly defined in the lattice theory that gives the atomic displacements at discrete lattice sites, which is a discrete variable. In order to interpret the experimental results, one needs a model to relate the discrete distortion near the point defect to measurable strains at or near the surface. Although elegant averaging techniques[14] have been developed for this purpose in infinite solids, the averaging process is not unique and requires careful attention to various conservation laws. In contrast, the MSGF method directly relates the lattice distortion to the measurable continuum parameters while it fully accounts for the discrete nature of the solid near the defect and includes the effect of the free surface on the lattice distortion.

The MSGF is based upon the fact[6,7] that the LSGF for a perfect lattice reduces asymptotically to the continuum Green's function (CGF). However, when a lattice has defects, its response is given by the defect LSGF, which is a solution of the Dyson equation. We show in the next section that the defect LSGF does not reduce to the CGF. In the MSGF method, we write the response of the defect lattice as a product of the perfect LSGF and an effective Kanzaki force.[6] The Kanzaki forces contain all the discrete-lattice effects and, for a point defect, are localized near the defect. This relation is exact within the standard assumptions of the Born von Karman model. We then use the asymptotic relationship between the perfect LSGF and the CGF to model the extended defects while retaining the atomistic effects exactly in the effective-force term.

First we calculate the lattice distortion due to a vacancy in an infinite solid using the LSGF for a million atom model crystallite. These calculations give the Kanzaki forces, relaxation energy, and the relaxation volume of the vacancy in an infinite solid. For calculation of the LSGF, we use the many-body interatomic potential extending up to 5th neighbors obtained by Cleri and Rosato[10] by using a tight binding model. This potential correctly reproduces[10] the measured values of many physical parameters of a perfect Cu lattice such as the elastic constants, phonon frequencies, etc. This potential has recently been used by Sandberg and Grimvall[15] to calculate the anharmonic contribution to the formation enthalpy of a vacancy in copper at high temperatures. As given in Sec. III, using this potential, our calculated value of the relaxation volume of a vacancy in Cu lattice agrees very well with the experimental value.[16] Of course this agreement in itself is not an indication that our method is working but it lends credence to our physical model.

The million-atom crystallite of the LSGF forms the core of the MSGF model. The core is treated atomistically. We then use the CGF for a semi-infinite anisotropic solid to calculate the change in the Kanzaki forces due to a free (100) surface in fcc Cu. The final values of the Kanzaki forces fully and exactly account for the discrete atomistic structure of the lattice near the vacancy and the effect of the free surface in the continuum limit. We use these values of the Kanzaki forces to calculate the strain and displacement fields at the free surface due to the vacancy and also the interaction energy between the vacancy and the free surface.

Calculations on a vacancy in an infinite Cu lattice have been carried out earlier by many authors (see, for example, Refs. 4–6, 17) using a pair interatomic potential. However, it is well known that a pair interatomic potential is unrealistic for a metal like Cu. Hence these calculations need to be revised. Several authors (for references, see Refs. 8 and 10) have used computer simulation methods and more realistic potentials to calculate the formation energy of a vacancy in an infinite Cu lattice for a small model crystallite consisting of a few hundred atoms. Cleri and Rosato[10] have used their potential to calculate the formation energy and the formation volume of a vacancy in infinite Cu using MD for a small crystallite containing 256 atoms.

Our calculated value of the formation energy of the vacancy in an infinite Cu lattice agrees with the value obtained by Cleri and Rosato.[10] However, they did not report the values of lattice distortion, relaxation energy and relaxation volume of the vacancy, which are important parameters. In addition, none of the published papers report calculations on strain and the displacement fields due to a point defect in a solid containing a free surface. Hence, there is a clear need for a multiscale model that can be used to calculate all these parameters.

Section II defines the LSGF and gives the formulation of the MSGF method. We give only the definition of the LSGF and refer the reader for the details of the LSGF method to our earlier papers.[6,7] Section III gives numerical results for a vacancy and free surface in a semi-infinite fcc Cu. Section IV gives a discussion of the MSGF and summarizes the main conclusions of the paper. Appendix A gives the CGF for an anisotropic semi-infinite Cu for the Mindlin problem[18–20] without derivation. Appendix B gives analytical expressions for force constants, change in force constants, and forces due to the vacancy and also the numerical values for near neighbor force constants and Green's functions for perfect fcc Cu. A preliminary report of this work assuming elastic isotropy and a crude model of force constants was presented at the Spring Meeting of the Materials Research Society.[21] Application of this technique to nanostructures such as quantum dots in semiconductors will be published elsewhere.

II. THEORY

We consider a monatomic Bravais lattice with a point defect at a lattice site. We assume a Cartesian frame of reference with the axes parallel to the crystallographic axes and the origin at a lattice site. We denote the lattice sites by vector indices $\mathbf{l}$, $\mathbf{l}'$, etc., and the Cartesian coordinates by indices i, j, k, etc. The lattice sites in the defect space will be denoted by $\mathbf{L}$, $\mathbf{L}'$, etc. that will be within the vector space of $\mathbf{l}$, $\mathbf{l}'$, etc. A vector index such as $\mathbf{l}$ has 3 components denoted by l_1, l_2, and l_3. The three-dimensional (3D) force constant matrix between atoms at $\mathbf{l}$ and $\mathbf{l}'$ is denoted by $\phi^*(\mathbf{l},\mathbf{l}')$. The force on atom $\mathbf{l}$ and its displacement from equilibrium position will be denoted, respectively, by $\mathbf{F}(\mathbf{l})$ and $\mathbf{u}(\mathbf{l})$, which are 3D column matrices. The displacement vector $\mathbf{u}(\mathbf{l})$ for atom at lattice site $\mathbf{l}$ gives the relaxation of the lattice or the lattice distortion caused by the defect.

By definition

$$[\Phi^*(\mathbf{l},\mathbf{l}')]_{ij} = \partial^2 W / \partial u_i(\mathbf{l}) \partial u_j(\mathbf{l}') \qquad (1)$$

and

$$[\mathbf{F}(\mathbf{l})]_i = -\partial W / \partial u_i(l), \qquad (2)$$

where W is the potential energy of the crystal and the derivatives in Eqs. (1) and (2) are evaluated at zero displacement. Following the method given in Refs. 6 and 7, we obtain

$$\mathbf{u}(\mathbf{l}) = \sum_{\mathbf{l}'} \mathbf{G}^*(\mathbf{l},\mathbf{l}')\mathbf{F}(\mathbf{l}'), \qquad (3)$$

where $\mathbf{G}^*$ is the defect lattice-statics Green's function. The lattice-statics Green's function is the zero-frequency limit of the phonon Green's function that has been extensively discussed in Ref. 22. Since our interest in this paper is only in the static response of the lattice, we will omit the qualifier "statics" for Green's function for brevity. The sum in Eq. (3) is over all lattice sites and Cartesian coordinates, which have not been shown explicitly for notational brevity.

In the representation of lattice sites, $\mathbf{G}^*$ and Φ^* are $3N$ $\times 3N$ matrices where N is the total number of lattice sites in the Born–von Karman supercell. The Green's function is formally given by

$$\mathbf{G}^* = [\Phi^*]^{-1}. \qquad (4)$$

For a perfect lattice in equilibrium without defects, $\mathbf{F}(\mathbf{l})$ is 0 for all $\mathbf{l}$, and the force constant and the Green's-function matrices have translational symmetry. We denote these matrices by Φ and $\mathbf{G}$, respectively. When a defect is introduced in the lattice, $\mathbf{F}(\mathbf{l})$ becomes, in general, nonzero and the force constant matrix changes. So

$$\Phi^* = \Phi - \Delta\Phi, \qquad (5)$$

where $\Delta\Phi$ denotes the change in the force-constant matrix Φ. From Eqs. (4) and (5), we obtain the following Dyson equation:

$$\mathbf{G}^* = \mathbf{G} + \mathbf{G}\Delta\Phi\mathbf{G}^*, \qquad (6)$$

where

$$\mathbf{G} = [\Phi]^{-1}, \qquad (7)$$

is the perfect lattice Green's function. In the same representation, we can write Eq. (3) as follows in the matrix notation:

$$\mathbf{u} = \mathbf{G}^*\mathbf{F}. \qquad (8)$$

Using Eq. (6), we rewrite Eq. (8) as

$$\mathbf{u} = \mathbf{G}\mathbf{F}^*, \qquad (9)$$

where

$$\mathbf{F}^* = \mathbf{F} + \Delta\Phi\mathbf{u}. \qquad (10)$$

Equation (8) is used to calculate lattice distortion in the LSGF method. Its detailed derivation has been given in Ref. 6. Equation (9), the alternative form of Eq. (8), gives the displacement in terms of the perfect-lattice Green's function and an effective force denoted by $\mathbf{F}^*$, the so called Kanzaki force.[6] From Eq. (10), we can identify it as the force due to the defect on relaxed lattice sites, in contrast to $\mathbf{F}$, that denotes the force at the original lattice site due to the defect. Equation (9) is applicable to any point defect such as a vacancy, an interstitial, or a substitutional impurity.

For the perfect lattice, $\mathbf{G}(\mathbf{l},\mathbf{l}')$ has translation symmetry and, therefore, can be labeled by a single index $\mathbf{l}$-$\mathbf{l}'$. It is calculated by using the discrete Fourier representation[6,22]

$$\mathbf{G}(\mathbf{l}) = (1/N) \sum_{\mathbf{q}} \mathbf{G}(\mathbf{q}) \exp[\iota\mathbf{q}.\mathbf{r}(\mathbf{l})], \qquad (11)$$

where $\iota = \sqrt{-1}$, $\mathbf{r}(\mathbf{l})$ is the radius vector for the lattice site $\mathbf{l}$, N is the total number of atoms

$$\mathbf{G}(\mathbf{q}) = [\Phi(\mathbf{q})]^{-1}, \qquad (12)$$

$\Phi(\mathbf{q})$ is the Fourier transform of the force constant matrix, and $\mathbf{q}$ is a vector in the reciprocal space of the lattice. For brevity of notation, we shall use the same symbol for a function and its discrete Fourier transform, the distinguishing feature being the argument of the function. Since $\mathbf{G}(\mathbf{q})$ and $\Phi(\mathbf{q})$

are 3×3 matrices, Eqs. (11) and (12) can be used to calculate the perfect-lattice Green's function $\mathbf{G}(\mathbf{l},\mathbf{l}')$.

The sum in Eq. (11) is over discrete values of $\mathbf{q}$ in the first Brillouin zone of the lattice. The symmetry of the lattice can be exploited to reduce the number of terms in the sum. For example, for cubic solids, it is necessary to carry out the sum over only 1/48th of the first Brillouin zone. For a million-atom model ($N = 10^6$) the calculation of $\mathbf{G}(\mathbf{l})$ takes only a few seconds on an ordinary 3 GHz desktop computer. Even a billion-atom model ($N = 10^9$) would take only about an hour of CPU time.

The solution of the Dyson's equation [Eq. (6)] is obtained by partitioning the matrices in the defect space and is described in Appendix B. After calculating $\mathbf{u}$ for all atoms in the defect space using Eq. (B42), we calculate Kanzaki force in the defect space by using Eq. (B43). The matrix $\Delta\Phi$ and the vectors $\mathbf{F}^*$ and $\mathbf{F}$ are 0 outside the defect space but not $\mathbf{u}$. The displacement of all other atoms in the solid is then given in terms of the perfect-lattice Green's function by use of Eq. (9). The Kanzaki force contains the full contribution of the discrete lattice structure in the defect space.

The LSGF expressions[6] for relaxation energy associated with the lattice distortion and the relaxation volume are given below:

$$W_{\text{rel}} = -\left(\frac{1}{2}\right) \sum_{\mathbf{L}} \mathbf{f}(\mathbf{L}) \cdot \mathbf{u}(\mathbf{L}) \tag{13}$$

and

$$\Delta V_{\text{rel}} = \text{Tr } \mathbf{D}/(c11 + 2c12), \tag{14}$$

where D is the dipole tensor defined by[6]

$$D_{ij} = \sum_{\mathbf{L}} f_i^*(\mathbf{L}) \cdot r_j(\mathbf{L}). \tag{15}$$

The summation in Eqs. (13) and (15) are over all atoms in the defect space. The relaxation energy is a part of the formation energy of the defect. Similarly, the relaxation volume is only a part of the formation volume of the defect.

The perfect-lattice Green's function varies[6] as $1/r(\mathbf{l})$ for large 1 and reduces asymptotically to the continuum Green's function. To establish the correspondence between the LSGF and CGF, we make $\mathbf{r}(\mathbf{l})$ and $\mathbf{q}$ continuous variables and replace the summation in Eq. (11) by integration over the reciprocal space. In conformity with the continuum model notation, we replace $\mathbf{r}(\mathbf{l})$ by $\mathbf{x}$ for large l, which will denote the position vector corresponding to the lattice site $\mathbf{l}$. Thus, in the limit $x \to \infty$

$$\mathbf{G}(\mathbf{x}) \cong \mathbf{G}_c(\mathbf{x}) = \left(\frac{1}{2\pi}\right)^3 \int \mathbf{G}_c(\mathbf{q}) \exp(\iota \mathbf{q} \cdot \mathbf{x}) d\mathbf{q}, \tag{16}$$

where, keeping terms up to q^2 in $\phi(\mathbf{q})$,

$$\mathbf{G}_c(\mathbf{q}) = \lim_{q \to 0} \mathbf{G}(\mathbf{q}) = \lim_{q \to 0} [\Phi(\mathbf{q})]^{-1} = [\Lambda(\mathbf{q})]^{-1}. \tag{17}$$

The subscript c on G in Eq. (16) denotes the Green's function in the continuum model. In Eq. (17), Λ is the Christoffel matrix, which is defined in terms of $\mathbf{c}$, the elastic constant tensor, as follows:

$$\Lambda_{ij}(\mathbf{q}) = c_{ikjl} q_k q_l. \tag{18}$$

Summation over repeated Cartesian indices is implied.

The asymptotic relation given by Eq. (16) is valid only for the perfect Green's function $\mathbf{G}$. It is generally not valid for the defect Green's function $\mathbf{G}^*$ defined by Eq. (4) unless the term containing $\Delta\Phi$ in Eq. (6) is negligible. In most cases of practical interest it is not negligible. For example, in the case of a vacancy $\Delta\Phi = \Phi$. Moreover, if the effect of $\Delta\Phi$ is negligible, then the information about the defect is lost. Calculations in this region are, therefore, not of interest for studying the properties of the defect.

In the earlier literature (for references, see Ref. 6) it has been often assumed that the $\Delta\Phi$ term in Eq. (6) is of higher order than the $\mathbf{G}$ term and will be negligible for large $|\mathbf{l} - \mathbf{l}'|$ even for large $\Delta\Phi$. This is not exactly right even though G varies as $1/r(\mathbf{l} - \mathbf{l}')$ for large $|\mathbf{l} - \mathbf{l}'|$. To see this, consider the response at $\mathbf{l}$ for a force at $\mathbf{l}'$ where $|\mathbf{l} - \mathbf{l}'|$ is large. The first term on the right of Eq. (6) is $\mathbf{G}(\mathbf{l},\mathbf{l}')$, which varies as $1/r(\mathbf{l} - \mathbf{l}')$ for large $|\mathbf{l} - \mathbf{l}'|$ and reduces to $\mathbf{G}_c$. The next term in the expansion of the right of Eq. (6) is $\mathbf{G}(\mathbf{l},\mathbf{l}'')\Delta\Phi(\mathbf{l}'',\mathbf{l}''')\mathbf{G}(\mathbf{l}''',\mathbf{l}')$. If the defect space is localized, such as in the case of a point defect, then $\mathbf{l}',\mathbf{l}'',\mathbf{l}'''$ are all close to each other and $|\mathbf{l}''' - \mathbf{l}'|$ is not large. Thus the second term on the right of Eq. (6) is of the same order in distance as the first term and will not be negligible unless $\Delta\Phi$ is negligible. The second term will be of a higher order in distance only if both $\mathbf{l}'$ and $\mathbf{l}$ are far away from the defect space. This case is not of much interest for modeling defects in lattices where the effect of the force due to the defect has to be calculated.

The advantage of writing the displacement in the form of Eq. (9) is now obvious. We can use the full power of continuum mechanics by using the continuum-model Green's function for $\mathbf{G}$ where needed while retaining the discrete lattice effects and all the characteristics of the defect exactly in $\mathbf{F}^*$.

Equation (9) is the master equation of our MSGF method. At large distances from the point defect and near extended defects, we replace $\mathbf{G}$ by the continuum Green's function defined by Eq. (17) but use the lattice value of $\mathbf{f}^*$ (or $\mathbf{F}^*$) as defined in terms of lattice Green's function by Eqs. (10) and (B42). Equation (9) is the multiscale representation of the defect since it relates the discrete lattice parameters through $\mathbf{f}^*$ to the continuum model parameters through $\mathbf{G}_c$. Thus the displacement field in our multiscale model at the position vector $\mathbf{x}$ for large x is given by the following sum over the defect space:

$$\mathbf{u}(\mathbf{x}) = \sum_{\mathbf{L}'} \mathbf{G}_c(\mathbf{x},\mathbf{L}') \mathbf{f}^*(\mathbf{L}'). \tag{19}$$

We can now incorporate the effect of extended defects in $\mathbf{G}_c$ by imposing appropriate boundary conditions using the standard techniques of the continuum model. As an example, we consider a semi-infinite solid with a free surface and calcu-

late the strains at the surface due to a vacancy in the bulk. We also calculate the displacement field at the free surface and the elastic interaction energy between the vacancy and the free surface. We choose a frame of reference in which the origin and the x and y axes are on the free surface and the positive z axis points into the solid. The axes are assumed to be parallel to the crystallographic axes. The zero-traction boundary condition at the free surface, which is taken to be the plane at $x_3 = 0$, is given by

$$\tau_{i3}(\mathbf{x}) = c_{i3jk}e_{jk}(\mathbf{x}) = 0 \quad (x_3 = 0), \tag{20}$$

where

$$e_{jk} = \partial u_j(\mathbf{x})/\partial x_k, \tag{21}$$

$\mathbf{e}$ and $\boldsymbol{\tau}$ denote, respectively, the second-rank strain and stress tensors, and $\mathbf{c}$ is the fourth-rank elastic-constant tensor. The off-diagonal elements of Eq. (21) have to be symmetrized in the definition of the strain tensor.

An expression for the $\mathbf{G}_c$ that satisfies Eq. (20) has been given in Appendix A without derivation. It is written as a sum of $\mathbf{G}_0$, the Green's function for the infinite solid, and $\mathbf{G}_s$, due to the contribution of the free surface, as follows:

$$\mathbf{G_c}(\mathbf{x},\mathbf{L}) = \mathbf{G_0}(\mathbf{x}-\mathbf{L}) + \mathbf{G_s}(\mathbf{x},\mathbf{L}), \tag{22}$$

where $\mathbf{L}$ is confined to the discrete lattice sites in the defect space. Equation (22) can be used if the point defect is far from the free surface. If $\mathbf{x}$ is close to the defect space, one should use the LSGF for $\mathbf{G_0}$ in Eq. (22) as given in Ref. 6 but the second term can still be used. Unlike the CGF for infinite solid, the LSGF is not singular at $\mathbf{x} = \mathbf{L}$. The second term, though derived from the continuum model, is not singular at $\mathbf{x} = \mathbf{L}$.

The strain field at $\mathbf{x}$ can be calculated by using Eq. (21). Equation (19) is equivalent to the solution of the Christoffel equation for a solid containing a discrete distribution of body forces $\mathbf{F}(\mathbf{L})$. It is also similar to the corresponding equation in the LSGF method[6] with $\mathbf{G}$ replaced by $\mathbf{G}_c$.

We now derive an expression for the elastic interaction energy between the point defect and the free surface. The total elastic strain energy for the solid is given by

$$W_{\mathrm{el}} = -\left(\frac{1}{2}\right) c_{ijkl} \int_V e_{kl}(\mathbf{x}) e_{ij}(\mathbf{x}) d\mathbf{x}, \tag{23}$$

where the integration extends over the whole volume of the solid. Using Eq. (21) and the Gauss theorem, we write Eq. (23) in the form

$$W_{\mathrm{el}} = -\left(\frac{1}{2}\right) c_{ijkl} \left[\int_S e_{kl}(\mathbf{x}) u_i(\mathbf{x}) n_j d\mathbf{x}_s \right.$$
$$\left. - \int_V (\partial^2 u_k(\mathbf{x})/\partial x_j \partial x_l) u_i(\mathbf{x}) d\mathbf{x} \right], \tag{24}$$

where the integral in the first term is over the surface of the solid and $\mathbf{n}$ is the surface normal. This term is 0 in view of Eq. (20). Using the Christoffel equation given in Appendix A, the second term on the right-hand side (rhs) of Eq. (24)

can be written in terms of the body forces. Thus, Eq. (24) reduces to the simple expression

$$W_{\mathrm{el}} = -\left(\frac{1}{2}\right) \sum_{\mathbf{LL}'} \mathbf{f^T}^*(\mathbf{L}) \mathbf{G_c}(\mathbf{L},\mathbf{L}') \mathbf{f}^*(\mathbf{L}'), \tag{25}$$

where we have replaced the volume integral by the sum over the defect space and the superscript T denotes matrix transpose.

The first term in $\mathbf{G}_c$ of Eq. (22), when used in Eq. (25), gives W_{rel}, the relaxation energy of the vacancy in the infinite solid. However, the use of the CGF is not justified for calculation of W_{rel}, because the discrete-lattice effects are important. It should be calculated by using the lattice Green's function[6] that gives Eq. (13). To calculate the interaction energy between the vacancy and the free surface, we use the CGF even if $\mathbf{l}$ and $\mathbf{l}'$ are both in the defect space if the distance between the vacancy and the free surface is large enough. The interaction energy between the vacancy and the free surface is obtained by using the second term of Eq. (22) into Eq. (25), and is given by

$$W_{\mathrm{int}} = -\left(\frac{1}{2}\right) \sum_{\mathbf{LL}'} \mathbf{f^T}^*(\mathbf{L}) \mathbf{G_s}(\mathbf{L},\mathbf{L}') \mathbf{f}^*(\mathbf{L}'). \tag{26}$$

Now, we consider the induced interaction between the surface and the vacancy. The induced interaction between two defects arises from the change in the Kanzaki force due to one defect by the presence of the other defect.[6] This interaction is of higher order and can be calculated by iteration. In the present case, the presence of the free surface induces additional displacements on the atoms in the solid. The displacements of the atoms in the defect space change the Kanzaki force and hence the strains at the surface as well as the interaction energy between the surface and the vacancy.

The first-order induced displacements on atoms in the defect space caused by the surface are given by

$$\Delta\mathbf{u}(\mathbf{L}) = \sum_{\mathbf{L}'} \mathbf{G_s}(\mathbf{L},\mathbf{L}') \mathbf{F}^*(\mathbf{L}'). \tag{27}$$

We then calculate the new Kanzaki force from Eq. (10) and use this value in the calculation of the strain and the interaction energy from Eqs. (19), (21), and (26). Higher order induced displacements and corrections to the strain and the interaction energy can be calculated by using Eq. (27) again with the new Kanzaki force and then further modifying the Kanzaki force.

Finally, Eq. (19) can also be used for calculating the effect of an applied surface stress on the defect. Since Eq. (19) expresses the response of the solid near the free surface in terms of the CGF, standard continuum mechanics[1–3] can be used for such calculations. For example, the interaction between the applied surface stress and the vacancy is given by an equation similar to Eq. (25) with $\mathbf{f^T}$ replaced by the applied stress, $\mathbf{L}$ replaced by the continuous variable $\mathbf{x}$, and taking the derivatives of $\mathbf{G_c}$ with respect to x.

III. APPLICATION TO FCC COPPER

For the purpose of illustration, we apply the MSGF method given in Sec. II to calculate the displacement field and strains at the free surface due to a vacancy in an aniso-tropic semi-infinite crystal of copper. We also use the MSGF method to calculate the interaction energy between the vacancy and the free surface. We chose copper because (i) it is a material of great interest as is apparent from a large number of publications on point defects in copper, (ii) a good interatomic potential is available, and (iii) strain due to a vacancy and its interaction with the free surface are important for many studies such as diffusion and electromigration in copper interconnects.

We use the tight-binding potential for copper, which has been given by Cleri and Rosato.[10] The CR model potential extends up to fifth neighbor. It is a many-body potential that depends upon the coordinates of all 79 atoms that are within fifth neighbor distance of an atom. The potential correctly reproduces many static and dynamic properties of the solid including the cohesive energy, phonon dispersion, and the elastic constants.

In their excellent paper, Cleri and Rosato[10] have applied their potential to calculate the formation energy of a vacancy in fcc copper. However, they have not reported the calculation of the lattice distortion due to the vacancy. Lattice distortion due to a defect is an important parameter that characterizes the defect and is responsible for the elastic field of the defect. The lattice distortion can, in principle, be measured by x-ray scattering, which is useful for verification of the model. Cleri and Rosato used the molecular dynamics method to model a crystallite of copper (and many other metals) containing 256 atoms. Since the defect space itself consists of 79 atoms, it is important to model a crystallite containing a much larger number of atoms for a reliable calculation of the lattice distortion. Too small a crystallite can introduce spurious size effects.

First we use the LSGF method to calculate the atomic displacements due to a vacancy in a million-atom model using the Cleri–Rosato potential. We calculate the relaxation energy of the vacancy and its relaxation volume in an otherwise perfect lattice with no free surface. Then we calculate the Kanzaki forces and use the MSGF method as described in Sec. II to calculate the displacement field and the strains at the free surface, and the interaction energy of the vacancy with the free surface.

In order to calculate the perfect-lattice Green's function we calculate the force constants using the Cleri–Rosato potential up to fifth neighbors. Analytical expressions for the force constants and their numerical values for a perfect copper lattice have been given in Appendix B. The force constants for atoms beyond fifth neighbors make negligible contribution to the Green's function and the lattice distortion. We calculate the Green's function between all pair of atoms in the defect space by using Eq. (11) with $N = 10^6$. Calculated values of the perfect Green's functions for up to fifth-neighbor atoms are also given in Appendix B. The computed values of the Green's function for more distant neighbors, which are needed for the present calculations, and a com-

puter program for calculating the Green's functions can be obtained from the author on request.

We assume that the vacancy is at the origin. Since each atom in this model interacts with all atoms up to its fifth neighbors, the defect space consists of 79 atoms—the vacancy and its 78 neighbors. Each matrix in Eq. (B41) is therefore 237×237, and the force and the displacement vectors in Eqs. (B42) and (B43) are 237-dimensional. Analytical expressions for the $\Delta\phi$ matrix elements between all pairs of atoms and the force vector **f** for all atoms in the defect space are given in Appendix B. Their numerical values are not given here because of space constraints but can be obtained from the author. However, for further application of the present formalism, knowledge of the Kanzaki forces is enough, which are given below for each atom in the defect space.

The crystal retains the cubic point-group symmetry in the presence of the vacancy if the point group operators are applied about the vacancy. In the present case, we can use group theory to reduce the 237×237 matrices in Eq. (B41) to 7×7 matrices, which simplifies the matrix inversion considerably. We use this procedure[6] to calculate the atomic displacements and Kanzaki forces, which are given below for atoms in the defect space. The results for other atoms in the defect space can be obtained by symmetry. All the lengths are in units of a, and the forces are in units of eV/a, where $2a = 3.61$ Å is the lattice constant of copper.

$$u(1,1,0) = \begin{bmatrix} -0.012 \\ -0.012 \\ 0 \end{bmatrix}, \quad F^*(1,1,0) = \begin{bmatrix} -0.308 \\ -0.308 \\ 0 \end{bmatrix}, \quad (28)$$

$$u(2,0,0) = \begin{bmatrix} 4.14 \\ 0 \\ 0 \end{bmatrix} * 10^{-3}, \quad F^*(2,0,0) = \begin{bmatrix} 0.081 \\ 0 \\ 0 \end{bmatrix}, \quad (29)$$

$$u(2,1,1) = \begin{bmatrix} -3.85 \\ -2.88 \\ -2.88 \end{bmatrix} * 10^{-3}, \quad F^*(2,1,1) = \begin{bmatrix} -3.77 \\ -2.04 \\ -2.04 \end{bmatrix} * 10^{-3}, \quad (30)$$

$$u(2,2,0) = \begin{bmatrix} -4.98 \\ -4.98 \\ 0 \end{bmatrix} * 10^{-3}, \quad F^*(2,2,0) = \begin{bmatrix} -9.61 \\ -9.61 \\ 0 \end{bmatrix} * 10^{-3}, \quad (31)$$

$$u(3,1,0) = \begin{bmatrix} 3.64 \\ -1.34 \\ 0 \end{bmatrix} * 10^{-4}, \quad F^*(3,1,0) = \begin{bmatrix} -4.16 \\ -1.59 \\ 0 \end{bmatrix} * 10^{-3}. \quad (32)$$

We see from Eq. (25) that the radial displacement of the nearest neighbor is about $0.017a = 0.003$ nm which is about 1% of the equilibrium value of the nearest neighbor distance. This shows that the lattice will be strained substantially near the defect. The relaxation energy and the relaxation volume of the vacancy in the infinite solid as calculated from Eqs. (13) and (14) are given below
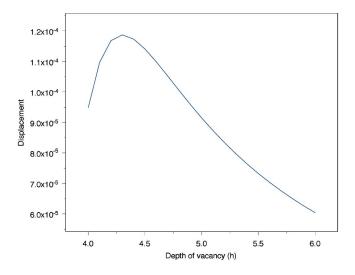
FIG. 1. The z component of the displacement at $(0,0,0)$ on the free surface due to a vacancy at $(0,0,h)$ in copper. All length are in units of $a = 1.805$ Å, half the lattice constant of fcc Cu.

FIG. 2. The diagonal components of strain at $(0,0,0)$ on the free surface due to a vacancy at $(0,0,h)$ in copper. Solid line—e11, dotted line—e33.

$$W_{rel} = -0.032 \text{ eV} \quad \text{and} \quad \Delta V_{rel}/V_a = -0.24, \quad (33)$$

where $V_a = 2a^3$ is the original volume of the monatomic fcc unit cell. Cleri and Rosato calculated the total formation energy, which includes the relaxation energy, of the vacancy to be 1.25 eV which agrees with our calculations. They did not calculate the relaxation energy or the relaxation volume of the vacancy. Our calculated value of the relaxation volume agrees very well with the experimental value of -0.25 reported in Ref. 16.

Now we use the multiscale representation given by Eq. (9) to calculate the displacement field and the strains at the free surface. We assume that the free surface is a (100) plane. Using the value of $\mathbf{f}^*$ given by Eqs. (28)–(32), we apply Kanzaki forces at all the atoms in the defect space. We assume that the vacancy is located at $(0,0,h)$. We then use Eq. (19) to calculate the displacement field at the free surface with $\mathbf{G}_c$ given by Eq. (A2) of Appendix A. The strains are calculated in terms of the derivatives of $\mathbf{G}_c$. Finally, we calculate the interaction energy between the vacancy and the free surface by using Eq. (26).

Figure 1 shows the displacement field at the origin at the free surface as a function of h, the depth of the vacancy below the free surface. Figure 2 shows the diagonal components of the strain tensor at the origin as function of h. Figure 3 shows the interaction energy between the free surface and the vacancy also as a function of h. The coordinates of the vacancy in all the three figures are $(0,0,h)$. All lengths are in units of a $= 1.805$ Å, half the lattice constant of fcc Cu. In all the figures the minimum value of h is 4. This is to ensure that the defect space of the vacancy does not touch the surface. Since the fifth neighbor distance from the vacancy is about 3.16, the atomistic structure of the surface will need to be modeled for $h < 4$.

The results given in Figs. 1–3 include the contribution of the surface induced displacements calculated by using Eq. (27). This contribution is small and its calculation converges within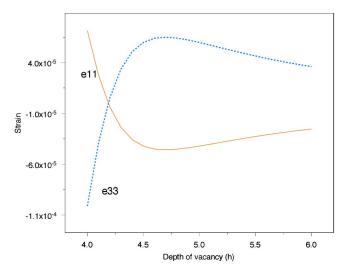 one iteration. An interesting effect of the surface in-duced displacements is on the displacement fields of those atoms where some of its components are 0 due to symmetry in the infinite lattice. The presence of the free surface destroys this symmetry and those components become nonvanishing. For example, the z component of the displacement of the atom at $(1,1,0)$ in the infinite lattice is 0 by symmetry. This component becomes nonzero when surface induced displacements are included. Overall, the maximum contribution of the surface displacement field (at $h = 4$) is less than 15% in Fig. 1, less than 4% in Fig. 2, and less than 0.1% in Fig. 3.

Figures 1 and 2 show an extremum near the surface. This extremum arises because of the boundary condition at the free surface given by Eq. (20), which forces certain combinations of the strain components to be 0. Overall the strain at the surface is small, that is, less than 0.01% for $h > 4$, but significant.
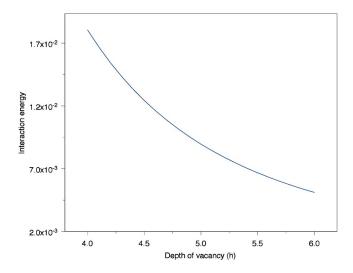

FIG. 3. The interaction energy between the vacancy and the free surface in copper. The interaction energy is units of the magnitude of the relaxation energy (0.032 eV) of the vacancy in infinite fcc Cu, which is calculated by using lattice statics Green's function.

The interaction energy is plotted in Fig. 3 in units of W_{rel}, the relaxation energy of a vacancy in an infinite solid. The value of W_{rel}, given in Eq. (33) is -0.032 eV. Figure 3 shows that W_{int}, the interaction energy of the vacancy with the free surface, is small, being less than 0.0007 eV which is about 2% of the relaxation energy for $h > 4$. This will change the vacancy concentration approximately by the factor $\exp(W_{int}/k_B T)$ where k_B is the Boltzmann constant and T the temperature. At room temperature this factor is about 1.03 that shows that the vacancy concentration near the free surface will change by about 3%. The interaction energy in Fig. 3 falls rapidly as h increases. This shows that the vacancy concentration will be almost independent of the depth of the vacancy.

When $h \approx 3.16$, a fifth neighbor of the vacancy will be at or close to the surface and the defect space of the vacancy will overlap with the free surface. A fully atomistic model is needed to model a point defect at or near the free surface. This would require a detailed knowledge of the atomic arrangements at and near the free surface. In such cases Eq. (19) is not valid. The validity of our model increases with increasing h. For any h, the reliability of our results lies between a pure continuum calculation and a pure lattice calculation of the semi-infinite lattice provided the lattice calculation has been carried out for a crystallite containing a large number of atoms. A lattice calculation using too small a crystallite may introduce spurious size effects.

IV. DISCUSSION AND CONCLUSIONS

We have developed a multiscale Green's function (MSGF) method and applied it to model a vacancy in a semi-infinite fcc copper lattice containing a free surface. We have calculated physical quantities at two length scales (atomistic and continuum) as summarized below.

At the continuum scale, we have calculated the strain and the displacement field at the free (100) surface as a function of h, the depth of the vacancy from the free surface. The displacement field at the free surface due to a single vacancy is less than $10^{-4}a$ and the strains at the free surface are less than 0.01% for $h > 4a$ where a is half the lattice constant of Cu. These values are obtained by relating the discrete lattice distortion in the core region around the vacancy to the continuum model parameters at the free surface where measurements can be made without any need for an arbitrary averaging algorithm.

Measurement of the strain field can be used to characterize the vacancy in Cu. The calculated value of the strain being less than 0.01% is rather small but can be measured by using modern techniques such as Kossel and pseudo Kossel techniques[23] and CBED (convergent beam electron diffraction)[24] that are suitable for small specimens. The Kossel and pseudo Kossel techniques can measure changes in lattice constants up to 10^{-5} nm[23] which correspond to strains less than 10^{-5}. The CBED can be used to measure[24] strains of the order of 10^{-4}. Such small strains may not be of much interest in bulk crystals but they are important in determining and modeling the mechanical response of nanostructures. For example, vacancies have been found to play important role

in determining the mechanical properties of nanoscale copper and also in copper interconnects in electronic devices (see Ref. 25 which also gives other references).

We have also calculated the interaction energy between the vacancy and the free surface. It decreases rapidly with h and is less than 0.0007 eV for $h > 4a$ which is about 2% of the relaxation energy of the vacancy in the infinite solid. The interaction energy between the free surface and the vacancy determines the concentration of vacancies near the free surface which is useful for modeling diffusion and other related processes that are important for technological applications such as the stability and reliability of copper interconnects in devices. In the present case, it is shown the interaction with the surface would change the vacancy concentration by less than 3% near the free surface at room temperature.

The MSGF model is not applicable if the vacancy is too close to the surface, that is, when the vacancy is within the range of interatomic interactions from the surface atoms. However, in that region, the elastic interaction is not important. It becomes a problem of surface reconstruction which is outside the scope of the present paper. Our calculations fully account for the discrete atomistic structure of the lattice near the vacancy along with the effect of the free surface in the continuum limit. Such calculations have not been reported in the literature. This is achieved in our MSGF method by seamlessly linking the subnano atomistic and macro continuum scales. The MSGF method treats a point defect at the atomistic level by using the LSGF and links it seamlessly to the CGF. The continuum part of the MSGF is used to model the macroscopic defects such as free surfaces and interfaces using the standard techniques of the anisotropic continuum model.

At the atomistic scale, we have done a purely discrete lattice calculation of the lattice distortion and related parameters for a vacancy in infinite Cu using the LSGF method and assuming a million-atom model crystallite. We find that the displacement of the atom which is the nearest neighbor of the vacancy is about 0.003 nm. This amounts to a substantial deformation of the solid near the vacancy which can be measured.[23,24] Earlier calculations using the LSGF or similar semi-analytic methods for a vacancy in infinite Cu used unrealistic pair potentials. We used the many-body potential obtained by Cleri and Rosato,[10] which depends upon the coordinates of 79 atoms and extends up to the fifth neighbor of each atom. This potential correctly reproduces several and static and dynamic properties of the perfect Cu lattice.

We have also calculated the relaxation energy (-0.032 eV) which is a part of the formation energy of the defect. For the infinite Cu lattice, our calculated value of the formation energy of the vacancy agrees with that given by Cleri and Rosato.[10] This is expected because the relaxation energy is not sensitive to the size of the crystallite. In addition, we calculated the relaxation volume ($-0.24 V_a$) of the vacancy where V_a is the volume of a monatomic unit cell. The relaxation volume of the vacancy agrees very well with the experimental value $-0.25 V_a$.[16]

Cleri and Rosato have not reported their calculated values of the lattice distortion and the relaxation volume. This may be partly because the conventional MD is mainly intended

for calculations of energy and not for strains. The strains depend upon long-range atomic displacements that are obviously sensitive to the size of the model crystallite. For example, in the present case, an atom (or effectively the vacancy) interacts directly with its 78 atoms (up to 5th neighbors). The model crystallite used in the MD calculations of Cleri and Rosato contains 256 atoms. Thus the radius of the crystallite is only about $(256/78)^{1/3} \approx 1.5$ times the range of the atoms that are directly interacting with the vacancy. It is usual to assume the periodic boundary conditions at the edge of the crystallite to simulate an infinite solid. This introduces spurious size effects on the calculated values of the atomic displacements for atoms beyond the first few neighbors which are too close to the boundary of model crystallite.

In this paper we have considered only a single vacancy. The method can be applied to small clusters of vacancies by calculating the appropriate Kanzaki forces. There is no need to recalculate the Green's function. This is one of the advantages of the MSGF method that the same Green's function can be used for different defects in the same host lattice.

The MSGF method is especially useful for interpreting and analyzing the elastic response of nanocrystals. In a mathematical model of nanocrystals, the point defects need to be modeled at the atomistic scale, whereas free surfaces and interfaces can be adequately modeled at a macroscopic scale. The continuum model is not reliable close to the point defects, where the discrete lattice effects of the crystal are very important (see, for example, Refs. 6 and 7). On the other hand, the lattice model becomes difficult for modeling surfaces and interfaces. This is partly because of the CPU requirements and partly because the interatomic potential near a free surface may be different than that in the bulk due to the surface effects on the electronic band structure. However, the macroscopic elastic effects near a surface and other extended defects can be well represented by the continuum model.[3] The MSGF model exploits this power of the continuum model.

To conclude:

(i)   We have calculated the discrete atomic displacements in the bulk, relaxation volume, strain and the displacement field at a free (100) surface due to a vacancy and its elastic interaction energy with the free surface in a semi-infinite anisotropic fcc copper by using a new MSGF method;

(ii) the MSGF method fully accounts for the discrete structure of the lattice in the bulk of the solid and is computationally efficient for modeling large crystallites. The calculation of the LSGF for a million-atom model crystallite requires only a few CPU seconds on a standard 3 GHz desktop;

(iii) the MSGF method bridges the length scales seamlessly from atomistic (subnano) to macro and relates the measurable macroscopic parameters of the continuum model to the discrete lattice parameters. This makes the MSGF especially suitable for modeling point defects in nanocrystals in which free surfaces and interfaces play important roles.

APPENDIX A: CONTINUUM GREEN'S FUNCTION FOR AN ANISOTROPIC SEMI-INFINITE SOLID

We give expression for the CGF of an anisotropic semi-infinite solid with a free (100) surface. For derivation and details, see Refs. 18–20. We define a 3D vector K in the reciprocal space similar to q in Eq. (20) where $K_1 = \cos(\theta)$; $K_2 = \sin(\theta)$; $-\infty \leqslant K_3 \leqslant \infty$ and $0 \leqslant \theta \leqslant 2\pi$. For notational convenience, we define a 2D vector χ and $\mathbf{r}$ in the subspace of $\mathbf{x}$ such that $\chi_1 = x_1$, $r_1 = R_1$, $\chi_2 = x_2$, and $r_2 = R_2$. We can thus write general 3D vectors $\mathbf{x}$ and $\mathbf{R}$ in real space as (χ, x_3). In an analogous manner, we also define the corresponding 2D vectors κ in the subspace of $\mathbf{K}$, such that $\mathbf{K} = (\kappa, K_3)$, where $\kappa_1 = K_1$ and $\kappa_2 = K_2$. In order to calculate the CGF, we need to solve the determinantal equation

$$|\Lambda(\kappa, K_3)| = 0. \qquad (A1)$$

for K_3 where Λ is the Christoffel matrix defined in Eq. (22). Equation (A1) has 6 roots that are functions of θ. We choose three roots Q_m ($m = 1,3$) which have positive imaginary parts. The CGF for the semi-infinite solid can be written[18–20] as follows:

$$\mathbf{G}_c(\mathbf{x}, \mathbf{R}) = \mathbf{G}_0(\mathbf{x} - \mathbf{R}) + \mathbf{G}_s(\mathbf{x}, \mathbf{R}), \qquad (A2)$$

where

$$\mathbf{G}_0(\mathbf{x} - \mathbf{R}) = \mathrm{Re}\left(\frac{1}{4\pi^2}\right)$$
$$\times \int d\theta \sum_m \mathbf{M}(\kappa, \bar{Q}_m) \bar{W}_m M_0(\kappa, Q_m, \mathbf{R}), \qquad (A3)$$

$$\mathbf{G}_s(\mathbf{x}, \mathbf{R}) = -\mathrm{Re}\left(\frac{1}{4\pi^2}\right)$$
$$\times \int d\theta \sum_{m,n} \mathbf{V}(\kappa, Q_m, Q_n) M_s(\kappa, Q_m, Q_n, \mathbf{R}),$$
$$(A4)$$

$$M_0(\kappa, Q_m, \mathbf{R}) = [\kappa.(\chi - \mathbf{r}) + \bar{Q}_m(x_3 - R_3) + \iota\varepsilon]^{-1}, \qquad (A5)$$

$$M_s(\kappa, Q_m, Q_n, \mathbf{R}) = [\kappa.(\chi - \mathbf{r}) + Q_m x_3 - \bar{Q}_n R_3 + \iota\varepsilon]^{-1}, \qquad (A6)$$

$$\mathbf{V}(\kappa, Q_m, Q_n) = \mathbf{M}(\kappa, Q_m)\mathbf{A}(\kappa)\mathbf{S}(\kappa, \bar{Q}_n)\mathbf{M}(\kappa, \bar{Q}_n)W_m\bar{W}_n, \qquad (A7)$$

$$\mathbf{A}(\kappa) = \left[\sum_m \mathbf{S}(\kappa, Q_m)\mathbf{M}(\kappa, Q_m)W_m\right]^{-1}, \qquad (A8)$$

$$S_{ij}(\kappa, K_3) = c_{i3jk} K_k, \qquad (A9)$$

$$W_m = 1 \Big/ \Big[2 c_{11} c_{44}^2 Q_m \prod_{n \neq m} (Q_m^2 - Q_n^2) \Big], \qquad (A10)$$

the overhead bar denotes complex conjugate, and $\mathbf{M}(\mathbf{K})$ is the matrix of cofactors of $\Lambda(\mathbf{K})$. The integral over θ in Eqs. (A2) and (A3) is carried out in the interval 0 to 2π which can be reduced by using symmetry.

APPENDIX B: FORCE CONSTANTS AND GREEN'S FUNCTIONS FOR PERFECT FCC COPPER, AND FORCES AND CHANGE IN FORCE CONSTANTS DUE TO A VACANCY IN THE DEFECT SPACE

We calculate the force constant and Green's-function matrices for a perfect fcc copper lattice using the CR many-body potential.[10] We also calculate the change in the force-constant matrices and forces on each atom in an imperfect copper lattice containing a single vacancy. These analytical expressions should be useful for modeling of defects in fcc lattices and have not been published before.

The energy of the atom $\mathbf{L}$ in the CR model is written as

$$W_{\mathbf{L}} = -\xi \sqrt{E_{\mathbf{L}}} + A P_{\mathbf{L}}, \qquad (B1)$$

where

$$E_{\mathbf{L}} = \sum_{\mathbf{L}' \neq \mathbf{L}} V_a(\mathbf{L}, \mathbf{L}'), \qquad (B2)$$

$$P_{\mathbf{L}} = \sum_{\mathbf{L}' \neq \mathbf{L}} V_r(\mathbf{L}, \mathbf{L}'), \qquad (B3)$$

$$V_a(\mathbf{L}, \mathbf{L}') = \exp{-2q[R(\mathbf{L}, \mathbf{L}')/d - 1]}, \qquad (B4)$$

$$V_r(\mathbf{L}, \mathbf{L}') = \exp{-p[R(\mathbf{L}, \mathbf{L}')/d - 1]}, \qquad (B5)$$

$$\mathbf{R}(\mathbf{L}, \mathbf{L}') = \mathbf{r}(\mathbf{L}') + \mathbf{u}(\mathbf{L}') - \mathbf{r}(\mathbf{L}) - \mathbf{u}(\mathbf{L}), \qquad (B6)$$

$R(\mathbf{L}, \mathbf{L}') = |\mathbf{R}(\mathbf{L}, \mathbf{L}')|$, $\mathbf{u}(\mathbf{L})$ is the instantaneous displacement of atom $\mathbf{L}$, $\mathbf{r}(\mathbf{L})$ is its position vector at equilibrium, and d is the nearest-neighbor distance. The values of the parameters for copper are: $\xi = 1.224$ eV, $A = 0.0855$ eV, $q = 2.278$, and $p = 10.96$. We write all the distances in units of $a = 1.805$ Å, half the lattice constant of copper, so that $d = \sqrt{2}$. The sums in Eqs. (B2) and (B3) extend over all atoms $\mathbf{L}'$ up to fifth-nearest neighbors.

The total energy W of the crystal is equal to the sum of W_L over all atoms $\mathbf{L}$. For a perfect lattice $E_{\mathbf{L}}$, $P_{\mathbf{L}}$, and $W_{\mathbf{L}}$ are all independent of $\mathbf{L}$. We denote the value of $E_{\mathbf{L}}$ for a perfect lattice by E_p for all $\mathbf{L}$. The elements of the force matrix (column vector) $\mathbf{F}(\mathbf{L})$ for atom $\mathbf{L}$ and the force constant matrix $\Phi(\mathbf{L}, \mathbf{L}')$ between atoms $\mathbf{L}$ and $\mathbf{L}'$ are defined as follows:

$$F_i(\mathbf{L}) = -\partial W / \partial u_i(\mathbf{L}) \qquad (B7)$$

and

$$\Phi_{ij}(\mathbf{L}, \mathbf{L}') = \partial^2 W / \partial u_i(\mathbf{L}) \partial u_j(\mathbf{L}'), \qquad (B8)$$

where the derivatives are evaluated at $\mathbf{u}(\mathbf{L}) = 0$ for all $\mathbf{L}$.

First, we evaluate the force constant matrix for the atoms $\mathbf{L}$ and $\mathbf{L}'$ as given by Eq. (B8). We neglect the interaction between atoms farther than the fifth-neighbor distance. The direct contribution to $\Phi(\mathbf{L}, \mathbf{L}')$ comes from $E_{\mathbf{L}}$ and $E_{\mathbf{L}'}$ ($\mathbf{L}' \neq \mathbf{L}$). In addition there are indirect contributions from all atoms that are within fifth-neighbor distance from both $\mathbf{L}$ and $\mathbf{L}'$. These contributions are given below.

Direct contributions from $E_{\mathbf{L}}$ and $E_{\mathbf{L}'}$:

$$\Phi_{ij}^L(\mathbf{L}, \mathbf{L}') = \xi C_{1\mathbf{L}}[\delta_{ij} V_{a1}(\mathbf{L}, \mathbf{L}') + \mathbf{D}(\mathbf{L}, \mathbf{L}')_{ij} V_{a2}(\mathbf{L}, \mathbf{L}')]$$
$$- A[\delta_{ij} V_{r1}(\mathbf{L}, \mathbf{L}') + \mathbf{D}(\mathbf{L}, \mathbf{L}')_{ij} V_{r2}(\mathbf{L}, \mathbf{L}')]$$
$$+ \xi C_{2\mathbf{L}}\Big[\sum_{\mathbf{L}'' \neq \mathbf{L}} R(\mathbf{L}, \mathbf{L}'')_i V_{a1}(\mathbf{L}, \mathbf{L}'') \Big]$$
$$\times R(\mathbf{L}, \mathbf{L}')_j V_{a1}(\mathbf{L}, \mathbf{L}'), \qquad (B9)$$

where

$$\mathbf{C}_{1\mathbf{L}} = \left(\frac{1}{2\sqrt{E_{\mathbf{L}}}} \right), \qquad (B10)$$

$$C_{2\mathbf{L}} = -\left(\frac{1}{4 E_L^{3/2}} \right), \qquad (B11)$$

$$\mathbf{D}(\mathbf{L}, \mathbf{L}')_{ij} = R(\mathbf{L}, \mathbf{L}')_i R(\mathbf{L}, \mathbf{L}')_j / R^2(\mathbf{L}, \mathbf{L}'), \qquad (B12)$$

$$V_{a1}(\mathbf{L}, \mathbf{L}'') = [1/R(\mathbf{L}, \mathbf{L}'')] dV_a(\mathbf{L}, \mathbf{L}'')/dR(\mathbf{L}, \mathbf{L}''), \qquad (B13)$$

$$V_{a2}(\mathbf{L}, \mathbf{L}') = -V_{a1}(\mathbf{L}, \mathbf{L}') + d^2 V_a(\mathbf{L}, \mathbf{L}'')/dR^2(\mathbf{L}, \mathbf{L}''), \qquad (B14)$$

δ_{ij} is the Kronecker's delta, and the sum in Eq. (B9) is over all atoms within fifth-neighbor distance of $\mathbf{L}$. The quantities V_{r1} and V_{r2} are defined by Eqs. (B11) and (B12) with V_a replaced by V_r. The contribution from $E_{\mathbf{L}'}$ is given by an equation similar to Eq. (B9) with $\mathbf{L}$ and i interchanged with $\mathbf{L}'$ and j, respectively.

Indirect contribution:

$$\Phi_{ij}^I(\mathbf{L}, \mathbf{L}') = -\xi \sum_{\mathbf{L}'' \neq \mathbf{L} \neq \mathbf{L}'} C_{2L''} R(\mathbf{L}'', \mathbf{L})_i V_{a1}(\mathbf{L}'', \mathbf{L})$$
$$\times R(\mathbf{L}'', \mathbf{L}')_j V_{a1}(\mathbf{L}'', \mathbf{L}'), \qquad (B15)$$

where the sum is over all atoms $\mathbf{L}''$ that are within fifth-neighbor distance of both $\mathbf{L}$ and $\mathbf{L}'$.

The total force constant matrix for the pair of atoms $\mathbf{L}$ and $\mathbf{L}'$ is given by

$$\Phi_{ij}(\mathbf{L}, \mathbf{L}') = \Phi_{ij}^L(\mathbf{L}, \mathbf{L}') + \Phi_{ij}^{L'}(\mathbf{L}, \mathbf{L}') + \Phi_{ij}^I(\mathbf{L}, \mathbf{L}'). \qquad (B16)$$

The force constant matrix for an atom with itself is obtained by using the condition[22]

$$\sum_{\mathbf{L}'} \Phi_{ij}(\mathbf{L}, \mathbf{L}') = 0. \qquad (B17)$$

For a perfect lattice $\mathbf{F}(\mathbf{L})=0$, E_L is independent of $\mathbf{L}$, and the sum in the third term on the right of Eq. (B9) is 0. For a perfect lattice, $\Phi(\mathbf{L},\mathbf{L}')$ depends only upon $\mathbf{L}'-\mathbf{L}$. The structure of these matrices is determined by the cubic symmetry of the fcc lattice.[6,22] The numerical results for the first 5 neighbors of the atom at the origin are given below in units of eV/a^2, where $a=1.805$ Å is half the lattice constant of copper.

$$\Phi(0;1,1,0)=-\begin{bmatrix} 3.322 & 3.603 & 0 \\ 3.603 & 3.322 & 0 \\ 0 & 0 & -0.319 \end{bmatrix}, \quad \text{(B18)}$$

$$\Phi(0;2,0,0)=-\begin{bmatrix} -2.847 & 0 & 0 \\ 0 & 0.063 & 0 \\ 0 & 0 & 0.063 \end{bmatrix}*10^{-1}, \quad \text{(B19)}$$

$$\Phi(0;2,1,1)=-\begin{bmatrix} -1.065 & -0.570 & -0.570 \\ -0.570 & -1.046 & 0.807 \\ -0.570 & 0.807 & -1.046 \end{bmatrix}*10^{-2}, \quad \text{(B20)}$$

$$\Phi(0;2,2,0)=-\begin{bmatrix} 1.691 & 1.733 & 0 \\ 1.733 & 1.691 & 0 \\ 0 & 0 & -0.121 \end{bmatrix}*10^{-2}, \quad \text{(B21)}$$

$$\Phi(0;3,1,0)=-\begin{bmatrix} 0.796 & 0.417 & 0 \\ 0.417 & -0.091 & 0 \\ 0 & 0 & -0.160 \end{bmatrix}*10^{-2}. \quad \text{(B22)}$$

Using the force-constant matrices given above, we calculate the perfect lattice static Green's function[6,7] using Eq. (11) for a million-atom model. The Green's-function matrices for the perfect lattice have exactly the same structure as the force-constant matrices. The calculated Green's function matrices for the first five neighbors are given below in units of a^2/eV. The calculated values for further neighbors can be obtained from the author on request.

$$G(0;0)=\begin{bmatrix} 7.648 & 0 & 0 \\ 0 & 7.648 & 0 \\ 0 & 0 & 7.648 \end{bmatrix}*10^{-2}, \quad \text{(B23)}$$

$$G(0;1,1,0)=\begin{bmatrix} 2.497 & 0.890 & 0 \\ 0.890 & 2.497 & 0 \\ 0 & 0 & 2.019 \end{bmatrix}*10^{-2}, \quad \text{(B24)}$$

$$G(0;2,0,0)=\begin{bmatrix} 1.195 & 0 & 0 \\ 0 & 1.383 & 0 \\ 0 & 0 & 1.383 \end{bmatrix}*10^{-2}, \quad \text{(B25)}$$

$$G(0;2,1,1)=\begin{bmatrix} 1.361 & 0.327 & 0.327 \\ 0.327 & 1.235 & 0.205 \\ 0.327 & 0.205 & 1.235 \end{bmatrix}*10^{-2}, \quad \text{(B26)}$$

$$G(0;2,2,0)=\begin{bmatrix} 1.294 & 0.531 & 0 \\ 0.531 & 1.294 & 0 \\ 0 & 0 & 0.951 \end{bmatrix}*10^{-2}, \quad \text{(B27)}$$

$$G(0;3,1,0)=\begin{bmatrix} 0.831 & 0.152 & 0 \\ 0.152 & 0.919 & 0 \\ 0 & 0 & 0.854 \end{bmatrix}*10^{-2}. \quad \text{(B28)}$$

Now we calculate the change in the force-constant matrices due to a vacancy in copper. We create the vacancy at the origin. This will make $E_\mathbf{L}$ dependent on $\mathbf{L}$ and $\Phi^*(\mathbf{L},\mathbf{L}')$ will depend upon both $\mathbf{L}$ and $\mathbf{L}'$ separately. We define the defect vector space consisting of the vacancy and all atoms up to its fifth neighbors. The defect space thus consists of 79 lattice sites including the vacant lattice site at the origin and will be of dimension $3\times 79=237$. For all atoms in the defect space $E_\mathbf{L}\neq E_p$ and will depend upon its distance from the vacancy. For all atoms outside the defect space $E_\mathbf{L}=E_p$.

Since there is no atom at the origin $\Phi^*_{ij}(0,\mathbf{L})=0$. From Eq. (5)

$$\Delta\Phi_{ij}(0,\mathbf{L})=\Phi_{ij}(0,\mathbf{L}). \quad \text{(B29)}$$

In the pair potential approximation, $\Delta\Phi_{ij}(\mathbf{L},\mathbf{L}')=0$ for $\mathbf{L}\neq\mathbf{L}'\neq 0$. In the present case of the many-body potential these matrices will not be 0. For the imperfect lattice $\Phi^*_{ij}(\mathbf{L},\mathbf{L}')$ is given by Eqs. (B9), (B15), and (B16) with the difference that $E_\mathbf{L}$ depends upon $\mathbf{L}$ and the sum in the third term on the right of Eq. (B9) is not 0 since $\mathbf{L}''$ does not include the origin. We add and subtract $\mathbf{L}''=0$ term to the sum, which gives

$$\sum_{\mathbf{L}''\neq\mathbf{L}\neq 0}\mathbf{R}(\mathbf{L},\mathbf{L}'')_i V_{a1}(\mathbf{L},\mathbf{L}'')=-R(\mathbf{L},0)_i V_{a1}(\mathbf{L},0). \quad \text{(B30)}$$

Using Eq. (B30) into Eq. (B9) gives $\Phi^{*\mathbf{L}}_{ij}(\mathbf{L},\mathbf{L}')$. There is no change in the term due to the repulsive part of the potential, which is a pair interaction. Thus we obtain

$$\Delta\Phi^L_{ij}(\mathbf{L},\mathbf{L}')=\xi\Delta C_{1\mathbf{L}}[\delta_{ij}V_{a1}(\mathbf{L},\mathbf{L}')$$
$$+\mathbf{D}(\mathbf{L},\mathbf{L}')_{ij}V_{a2}(\mathbf{L},\mathbf{L}')]$$
$$-\xi C_{2\mathbf{L}}\mathbf{r}(\mathbf{L})_i V_{a1}(\mathbf{L},0)R(\mathbf{L},\mathbf{L}')_j V_{a1}(\mathbf{L},\mathbf{L}'), \quad \text{(B31)}$$

where

$$\Delta C_{1\mathbf{L}}=C_{1p}-C_{1\mathbf{L}} \quad \text{(B32)}$$

and

$$C_{1p}=\left(\frac{1}{2\sqrt{E_p}}\right). \quad \text{(B33)}$$

Similarly, we calculate the contribution $\Phi^{*\mathbf{L}'}(\mathbf{L},\mathbf{L}')$. The indirect contribution to the force-constant matrix is given by Eq. (B15). The difference from the perfect lattice term arises because $E_{\mathbf{L}''} \neq E_p$ and, in the imperfect case, the sum over $\mathbf{L}''$ does not include the origin. We obtain

$$\Delta\Phi_{ij}^{I}(\mathbf{L},\mathbf{L}') = -\xi\left[\sum_{\mathbf{L}''}{}' \Delta C_{2\mathbf{L}''} R(\mathbf{L}'',\mathbf{L})_i V_{a1}(\mathbf{L}'',\mathbf{L})\right.$$

$$\times R(\mathbf{L}'',\mathbf{L}')_j V_{a1}(\mathbf{L}'',\mathbf{L}')$$

$$\left. + C_{2p} r(\mathbf{L})_i V_{a1}(0,\mathbf{L}) r(\mathbf{L}')_j V_{a1}(0,\mathbf{L}')\right],$$
$$(B34)$$

where $\mathbf{L} \neq \mathbf{L}' \neq \mathbf{L}'' \neq 0$,

$$C_{2p} = -\left(\frac{1}{4\sqrt{E_p^{3/2}}}\right) \qquad (B35)$$

and

$$\Delta C_{2\mathbf{L}} = C_{2p} - C_{2\mathbf{L}}. \qquad (B36)$$

The prime over the summation sign on the right of Eq. (B34) denotes that the summation is carried out only over all the atoms in the defect space. The total $\Delta\Phi(\mathbf{L},\mathbf{L}')$ is obtained by the sum of all the contributions as in Eq. (B16). Finally, the change in the force constant matrix for an atom with itself is obtained by imposing the condition of invariance against rigid body translation given by Eq. (B17).

In the case of a perfect lattice, since the crystal has translational as well as inversion symmetry, the 3×3 force constant matrix between a pair of atoms is symmetric. For the imperfect case, the change in the force constant matrix between the vacancy and an atom is symmetric in view of Eq. (B29). In general, this matrix between other pairs of atoms is not symmetric. The lattice retains the whole point-group symmetry if the point-group operators are applied about the vacancy. The matrices in the defect space can, therefore, be block diagonalized by using the operators of the cubic point group as given in Ref. 6 and reduced to 7×7 matrices.

Finally, we calculate the forces on all atoms in the defect space by using Eq. (B7). The direct contribution to $\mathbf{F}^{\mathbf{L}}(\mathbf{L})$ the force on atom $\mathbf{L}$ comes from $E_{\mathbf{L}}$ and the indirect contribution $\mathbf{F}^{I}(\mathbf{L})$ comes from all atoms $\mathbf{L}''$ which are within fifth neighbor distance from $\mathbf{L}$. There is no atom at the origin. Following the steps similar to those for calculating the force constants, we obtain

$$\mathbf{F}_i^{\mathbf{L}}(\mathbf{L}) = -\xi C_{1\mathbf{L}} r(L)_i V_{a1}(0,\mathbf{L}) + A r(L)_i V_{r1}(0,\mathbf{L})$$
$$(B37)$$

and

$$\mathbf{F}_i^{I}(\mathbf{L}) = -\xi\left[\Delta C_{1\mathbf{L}} \sum_{\mathbf{L}' \neq \mathbf{L} \neq 0}{}' V_{a1}(\mathbf{L}',\mathbf{L}) R(\mathbf{L}',\mathbf{L})_i\right.$$

$$\left. + C_{1p} V_{a1}(0,\mathbf{L}) r(\mathbf{L})_i\right], \qquad (B38)$$

where the summation is restricted to the defect space. The total force on atom $\mathbf{L}$ is given by

$$\mathbf{F}_i(\mathbf{L}) = \mathbf{F}_i^{\mathbf{L}}(\mathbf{L}) + \mathbf{F}_i^{I}(\mathbf{L}). \qquad (B39)$$

We shall now give the solution[6] of the Dyson's equation. The forces by Eq. (B39) are 0 outside the defect space. Hence we can solve Eq. (6) by using the matrix partitioning technique[6,7,22] in the defect space. The matrix $\Delta\Phi$ is also 0 outside the defect space. The reduced Dyson equation[6,7,22] in the defect space is given by

$$\mathbf{g}^* = \mathbf{g} + \mathbf{g}\Delta\phi\mathbf{g}^*, \qquad (B40)$$

where $\mathbf{g}$, $\mathbf{g}^*$, and $\Delta\phi$ are, respectively, the blocks of $\mathbf{G}$, $\mathbf{G}^*$, and $\Delta\Phi$ in defect space. The matrices in Eq. (B40) are $3n \times 3n$ matrices, where n is the number of atoms in the defect space. For point defects, n is small so Eq. (B40) can be solved by direct matrix inversion, as given below.

$$\mathbf{g}^* = (\mathbf{I} - \mathbf{g}\Delta\phi)^{-1}\mathbf{g}, \qquad (B41)$$

where $\mathbf{I}$ is the unit matrix.

For example, for an fcc lattice with a short-range interatomic potential in which the defect interacts up to its second neighbor atoms, the matrices in Eq. (B41) are 57×57. Since a point defect such as a vacancy retains the local point-group symmetry of the lattice, we can use group theory to simplify Eq. (B41) considerably. In the case of a vacancy in an fcc lattice with second neighbor interaction, Eq. (B41) can be reduced to a 2×2 matrix equation.[6] In this paper we have assumed a many-body potential in which each atom interacts with up to its fifth neighbors. In this case the matrices in Eq. (B41) are 237×237. By using group theory, these matrices can be reduced to 7×7.

By definition, the force matrix defined by Eq. (2) is nonvanishing only in the defect space. Using Eqs. (8) and (B40), we obtain for all atoms in the defect space

$$\mathbf{u} = \mathbf{g}^* \mathbf{f}, \qquad (B42)$$

where $\mathbf{f}$ is the component of $\mathbf{F}$ in the defect space. The Kanzaki force in the defect space is given by

$$\mathbf{f}^* = \mathbf{f} + \Delta\phi\mathbf{u}. \qquad (B43)$$

---

*Electronic mail: tewary@boulder.nist.gov

[1] T. Mura, *Micromechanics of Defects in Solids* (Martinus Nijhoff Publishers, The Hague, 1982).

[2] J. D. Eshelby, *Solid State Physics*, edited by F. Seitz and D. Turnbull (Academic, New York, 1956), Vol. 3, p. 79.

[3] T. C. T. Ting, *Anisotropic Elasticity* (Oxford University Press, Oxford, 1996).

[4] R. Bullough and J. R. Hardy, Philos. Mag. **17**, 833 (1968).

[5] R. Bullough, M. J. Norgett, and S. Webb, J. Phys. F: Met. Phys. **1**, 345 (1971).

[6] V. K. Tewary, Adv. Phys. **22**, 757 (1973).

[7] R. Thomson, S. Zhou, A. E. Carlsson, and V. K. Tewary, Phys. Rev. B **46**, 10 613 (1992).

[8] M. Ortiz and R. Phillips, Adv. Appl. Mech. **36**, 1 (1999).

[9] P. Vashishta, A. Nakano, and R. K. Kalia, Mater. Sci. Eng., B **37**, 56 (1996).

[10] F. Cleri and V. Rosato, Phys. Rev. B **48**, 22 (1993).

[11] E. B. Tadmor, M. Ortiz, and R. Phillips, Philos. Mag. A **73**, 529 (1996).

[12] S. Rao, C. Hernandez, J. P. Simmons, T. A. Parthasarathy, and C. Woodward, Philos. Mag. A **77**, 231 (1998).

[13] R. Phillips, Curr. Opin. Solid State Mater. Sci. **3**, 526 (1998).

[14] J. Cormier, J. M. Rickman, and T. J. Delph, J. Appl. Phys. **89**, 99 (2001).

[15] N. Sandberg and G. Grimvall, Phys. Rev. B **63**, 184109 (2001).

[16] H. J. Wollenberger, *Physical Metallurgy*, 4th ed., edited by R. W. Cahn and P. Haasen (North-Holland, Amsterdam, 1996), Vol. II, p. 1622.

[17] A. G. Crocker, M. Doneghan, and K. W. Ingle, Philos. Mag. A **41**, 21 (1980).

[18] E. Pan, Proc. R. Soc. London **458**, 181 (2002).

[19] E. Pan and F. G. Yuan, Int. J. Solids Struct. **37**, 5329 (2000).

[20] E. Pan and B. Yang, J. Appl. Phys. **90**, 6190 (2001).

[21] V. K. Tewary, *Modeling and Numerical Simulation of Materials Behavior and Evolution*, edited by A. Zavaliangos, V. Tikare, and E. Olevsky (Materials Research Society, Warrendale, PA, 2002), p. 21.

[22] A. A. Maradudin, E. W. Montroll, G. H. Weiss, and I. P. Ipatova, *Theory of Lattice Dynamics in the Harmonic Approximation, Solid State Physics*, 2nd ed., edited by H. Ehrenreich, F. Seitz, and D. Turnbull, Suppl. 3 (Academic, New York, 1971).

[23] S. Däbritz, E. Langer, and W. Hauffe, Appl. Surf. Sci. **179**, 38 (2001).

[24] S. Kramer, J. Mayer, C. Witt, A. Weickenmeier, and M. Ruhle, Ultramicroscopy **81**, 245 (2000).

[25] Win-Jin Chang, Microelectron. Eng. **65**, 239 (2003).